Thermal Behavoiur of Valsartan Active Substance and in Pharmaceutical Products

IOANA CRISTINA TITA[1], BOGDAN TITA[2]*, CLAUDIA CRINA TOMA[2], ELEONORA MARIAN[3], LAURA VICAS[1,3]

[1] Carol Davila University of Medicine and Pharmacy, Faculty of Pharmacy, 6 Traian Vuia Str., 020956, Bucharest, Romania

[2] Vasile Goldis Western University of Arad, Faculty of Pharmacy, Department of Pharmaceutical Sciences, 86 L. Rebreanu Str., 300041, Arad, Romania

[3] University of Oradea, Faculty of Medicine and Pharmacy, Speciality of Pharmacy, 29 Nicolae Jiga Str., 410028, Oradea, Romania

TG/DTG and DSC curves provide important information regarding the physical properties of the pharmaceutical compounds (stability, compatibility, polymorphism, kinetic analysis, phase transitions etc). The thermal behaviour of valsartan was studied under dynamic nitrogen atmosphere, in comparison with pharmaceutical products containing the corresponding active substances. Also, the FT–IR spectra and X-ray diffactogram of the same samples were recorded. The main conclusion of this comparative study was that TG / DTG and DSC assays along with FT-IR spectra and X-ray diffractograms provide credible data for differences between active substance and pharmaceutical forms.

Keywords: valsartan, active substance, pharmaceutical product, TG/DTG/DSC, FT-IR, X-ray

One of the most common affections of today's lifestyle is arterial hypertension, one third of the population suffering from this disease [1,2].

Outpatient studies to monitor blood pressure have confirmed that blood pressure depends on the circadian phase. In people with normal blood pressure and uncomplicated essential hypertension, blood pressure drops to the lowest levels during night time sleep, increases steeply in the morning with awakening and reaches peak values during the first hours of diurnal activity. So it is very important to take the antihypertensive drugs [3-6].

Valsartan (S)-3-methyl-2-(N-{[2'-(2H-1,2,3,4-tetrazol-5-yl)biphenyl-4-yl]methyl} pentanamido)butanoic acid has the empirical formula $C_{24}H_{29}N_5O_3$ and a molecular mass of 435.519 g/mol (fig. 1) [7,8].

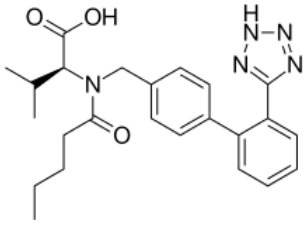

Fig. 1. Chemical structure of Valsartan

Valsartan is a very selective angiotensin II antagonist. It is active orally and acts on the AT1 receptor subtype [9]. It decreases blood pressure and improves blood flow by relaxing blood vessels. The solubility of valsartan in water is low (0.18 mg / mL) thus having a low oral bioavailability (~ 23%) [10,11].

Valsartan is a drug that is part of the angiotensin receptor blocker class. It works by blocking competitively binding angiotensin to its receptor in blood vessels. Studies have shown that agonist receptor blockers have been shown to be more effective compared to angiotensin converting enzyme inhibitors. Antihypertensive action is enhanced by calcium channel blockers [12-15].

Thermogravimetric analysis is an analytical method that produces rapid and reproducible results. This method is used for quality control of the drug through technological parameters, thus improving the end product. [16-19].

Differential scanning calorimetry is a more and more used method instead of differential thermal analysis. The method is used in identifying and determining the purity of active substances, but in particular, to evaluate the interaction of the substances from which the drugs are made. This method offers fast efficient results. [20-23].

In our previous research we have demonstrated the importance and utility of thermal analysis methods in predicting thermal stability and compatibility of different active substances with excipients or between them [24-30].

We have done this research because in the literature there are not many studies about thermal behaviour of the active substances compared to the pharmaceutical products containing this active substance. Studies on the compatibility of active substances with excipients are relatively low.

Our goal in this study was to compare the thermal behaviour of the active substance - valsartan with pharmaceuticals. Another goal was to determine accurately the melting point with the differential scanning calorimetry method, which is a criterion for controlling the purity of the substance.

FT-IR spectra and X-ray diffractograms were recorded for the pure substance and the pharmaceutical products to confirm the resulting differences from the TG / DTG and DSC curves of the analysed samples.

Experimental part

Materials and methods

The substances examined by thermal analysis, FT-IR spectroscopy and X-ray analysis were valsartan - active substance (V-AS) and two pharmaceutical products (P1, P2)

The active substance was obtained from Polisano Pharma SRL, Romania, lot: VT0020911 as pure compound, able to be used for medical purposes.

The pharmaceuticals (drugs) were commercial products, containing different excipients.

Thermal analysis

The TG/DTG and DTA curves were recorded using a Netzsch-STA 449 TG/DTA instrument in the temperature range 20-1000 °C, under a dynamic atmosphere of nitrogen (20 mL·min^{-1}) and at a heating rate (β) 10 °C·min^{-1}, using platinum crucibles and weighed ≈ 20 mg of samples.

* email: bogdantita@yahoo.com

Fourier transformed infrared spectroscopy (FT-IR) and X-ray diffraction

FT-IR spectra were recorded on a Shimadzu Prestige – 21 apparatus using KBr discs in the range 4000-400 cm^{-1}.

X-ray diffraction patterns (XRPD) were obtained with a Rigaku Ultima IV diffractometer ($Cu_{K\alpha}$ radiation).

Results and discussions

Thermal behaviour

Some of the thermoanalytical curves for the studied compounds, obtained under dynamic temperature conditions at heating rate (β) of 10 °C·min^{-1} and a nitrogen atmosphere, are presented in figures 2-4.

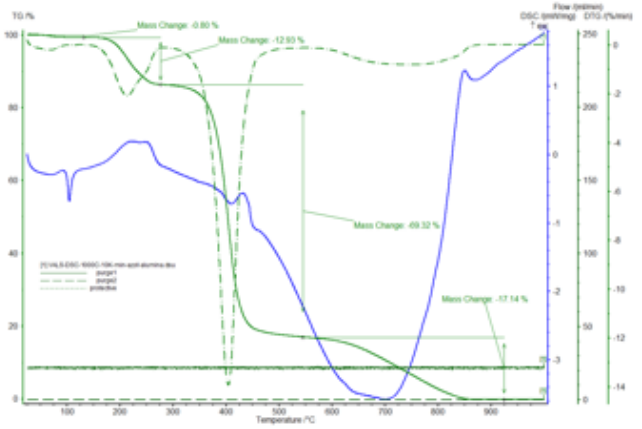

Fig. 2. TG/DTG and DSC curves of V-AS

Fig. 3. TG/DTG and DSC curves of P1

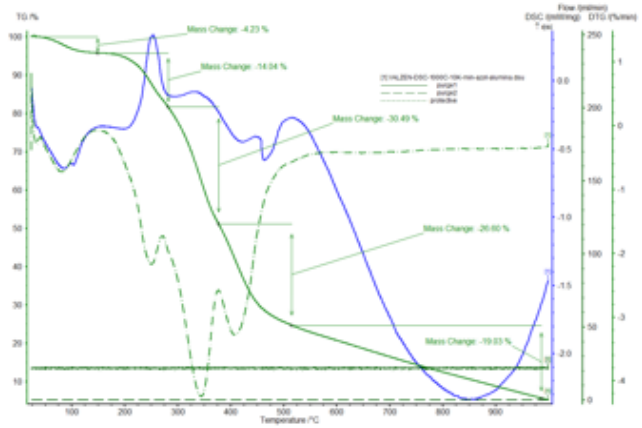

Fig. 4. TG/DTG and DSC curves of P2

According to the TG / DTG curves, V-AS eliminates the absorbed water (Δm = 1.10%) between temperatures 25.0 -131.3 °C, with $T_{peak\ DTG}$ = 70.0 °C. On the DSC curve, for the mentioned temperature range there appears an endothermic peak, ascutit, with $T_{peak\ DSC}$ = 107.5°C, which corresponds to melting.

V-AS is thermally stable up to 163.0 °C when its decomposition begins, which is going on three distinct successive processes.

Between temperatures 163.0-273.4 °C takes place the first decomposition process, with $T_{peak\ DTG}$ = 214.8 °C and Δm = 2.80%. This process is accompanied on the DSC curve by a small endothermic peak ($T_{peak\ DSC}$ = 235.5 °C).

The highest mass loss (Δm = 68.5%) occurs in the temperature range 273.4 – 544.4 °C ($T_{peak\ DTG}$ = 403.7). The decomposition process is of endothermic nature, on the DSC curve showing the corresponding peak, relatively small, with $T_{peak\ DSC}$ = 412.6 °C.

The last decomposition process, characterized by a broad decomposition peak on DSC curve and with $T_{peak\ DSC}$ = 700.0 °C, takes place in the temperature range of 544.4 – 870.4 °C and $T_{peak\ DTG}$ = 700.0°C. The mass loss (Δm) is 17.6%.

The heating behavior of the pharmaceutical products is relatively different in comparison to the active substance.

The TG/DTG curves of P1 (fig. 3) indicate the presence of four processes that occur during heating.

The first process takes place in the temperature range 50.0 - 129.9 °C, with $T_{peak\ DTG}$ = 70.1°C, and Δm = 3.80%. This process corresponds to the loss of moisture and water present in excipients such as microcrystalline cellulose, croscarmellose sodique. The process is accompanied by a strong endothermic effect with $T_{peak\ DSC}$ = 70.1°C, accompanied by a shoulder at 103.4 °C, corresponding to the melting process.

The next process is in the range of 129.9 – 275.0 °C, with $T_{peak\ DTG}$ = 207.5 °C and Δm = 8.4%. In this process, water is removed from lactose monohydrate and thermal decomposition begins: AS and excipients. The nature of the processes that occur from the thermal point of view is complex. This is due to the presence of the excipients, but also to their possible interactions with the active substance. Thus, on the DSC curve there appears a small endothermic peak, with $T_{peak\ DSC}$ = 225.0 °C, followed by a exothermic peak with $T_{peak\ DSC}$ = 252.2 °C.

The decomposition process with the highest mass loss Δm = 64% occurs in the temperature range 275.0 – 525.0 °C, $T_{peak\ DTG}$ = 359.7 °C, accompanied by a shoulder at 403.7 °C. The complex nature of the decomposition process is supported by the presence of the four peaks on the DSC curve. The first, small, endothermic type with $T_{peak\ DSC}$ = 300.0 °C is followed by a higher endothermic peak, with $T_{peak\ DSC}$ = 354.5 °C. The third, exothermic nature is the highest heat effect, and $T_{peak\ DSC}$ = 394.0 °C. Fourth peak, with $T_{peak\ DSC}$ = 434.3 °C is a bit sharp, of endothermic nature.

Thermal decomposition continues over a wider temperature range, 525.0 – 970.1 °C, with a peak DTG wide and $T_{peak\ DTG}$ = 751.8 °C, and mass loss is Δm = 23.8%. The complexity of the decomposition process is supported by the presence of two endothermic peaks on the DSC curve, with $T_{peak\ DSC}$ = 561.2 °C, respectiv $T_{peak\ DSC}$ = 892.6 °C.

Similarly, the thermal decomposition of P2 is a complex one.

The TG/DTG curves (fig. 4) show a first mass loss (Δm = 4.90%) in the temperature range 25.0 -150.0 °C, with $T_{peak\ DTG}$ = 85.2 °C. The mass loss corresponds to the water absorbed and excipient water (especially microcrystalline cellulose). The DSC curve shows an endothermic peak ($T_{peak\ DSC}$ = 92.6 °C), accompanied by another endothermic peak (shoulder) with $T_{peak\ DSC}$ = 103.6 °C and which corresponds to melting.

The next four stages of decomposition are difficult to delimit on the TG curve. In a first stage, corresponding to the temperature range 150.0 -268.1 °C, with $T_{peak\ DTG}$ = 250.0 °C and Δm = 13.8%, thermal decomposition begins, as well as the elimination of water from lactose monohydrate. Two peaks appear on the DSC curve: one endothermic,

V-AS	P1	P2	Assignement
3426 w	3424 w	3416 w	ν_{OH}(COOH); ν_{NH}(N-H)
2965-2874-2745-2616 m	2963-2922-2874 i-m	2963-2922-2872 m	$\nu_{asymC-H}$(CH_3;CH_2) ν_{symC-H}(CH_3;CH_2)
1732 m	1734 m	1726 m	$\nu_{C=O}$
1603 i	1603 i	1645 ; 1607 i	$\nu_{C=N}$; $\nu_{C=O}$
1470 m ; 1410 m	1468 m ; 1414 m	1466 m ; 1420 m	$\nu_{asymCOO}$; ν_{symCOO}; $\nu_{N=N}$
1274 m; 1206 m; 1165 m	1275 m; 1206 m; 1163 m	1277 m; 1206 m; 1167 m	ν_{C-N}; $\delta_{asym}CH_3$;CH_2;CH $\delta_{sym}CH_3$;CH_2;CH
1105 w; 1057 w	1107 w; 1059 w	1105 w; 1057 w	ν_{C-O}; ν_{C-C-O}; $\nu_{C-C(=O)-O}$ in p. C-H bend
997 w ; 939 w	999 w ; 939 w	999 m	o.p. C-H bend
853 w ; 816 w	853 w ; 816 w	851 w ; 816 w	ν_{Si-O}; o.p. C-H (ring)
758 m	758 m	758 m	o.p. C-H bend
677 w	677 w	669 w	o.p. (ring) C=C bend o.p. N-H bend o.p. O-H bend
563 w ; 515 w	561 w ; 519 w	561 w ; 519 w	o.p. C-H benzene substituted

Table 1
THE MAIN ABSORPTION BANDs (cm^{-1}) FOR THE STUDIED COMPOUNDS

relatively small, with $T_{peak\ DSC}$ = 200.0 °C and one exothermic, more pronounced, with $T_{peak\ DSC}$ = 256.2 °C.

The following process, is in the temperature range 268.1 – 381.5 °C and $T_{peak\ DTG}$ = 348.7°C, shows the highest mass loss (Δm = 30.0%). The process is of an endothermic nature, with $T_{peak\ DSC}$ = 300.0°C.

The decomposition continues, with successive and/or concurrent processes. In the temperature range of 381.5 – 514.8 C, with $T_{peak\ DTG}$ = 408.2°C, a mass loss of 26.5% occurs. The DSC curve shows two endothermic peaks: the first relative small with $T_{peak\ DSC}$ = 425.0 °C, respectively the second with $T_{peak\ DSC}$ = 465.7 °C.

The last decomposition step corresponds to a mass loss of 24.8%, and the final residue mass is zero. This occurs in the temperature range of 514.8-1000.0°C and is accompanied by DSC curves of a strong endothermic effect with $T_{peak\ DSC}$ = 850.0 °C.

Spectroscopy FT-IR

FT-IR spectroscopy is a very common technique used to determine possible interactions between active substance and excipients. Its role is to confirm the results obtained by thermal analysis. One of the reasons why it is increasingly used in drug analysis is that during the preparation of samples, the analyte does not undergo mechanical or thermal changes.

The proof of the interaction between substances can be demostrated highlighting the differecens between the FT-IR spectra, may it be with the appearance or dissapearance of new absorbtion bands or the increasing or decreasing in intensity.

The FT-IR spectra are presented in figure 5 and the main absorption bands are summarized in table 1.

The main differences resulting from comparing the spectrum of V-AS with the spectra of P1 and P2 are presented below, as follow:

– the broadening and the increase (≈ 15% for P1 and P2) of the bands from the region 3600-3200 cm^{-1}, attributed to the NH group present in the V-AS molecule, respectively to the OH group present in the V-AS molecule (carboxyl group) as well as in the excipients: starch, microcrystalline cellulose, lactose monohydrate, croscarmellose;

– the increase (≈ 10% for P1), respectively the decrease (≈ 15% for P2) of the intensity for the three bands from the region 3200 – 2400 cm^{-1} that correspond to the methylene, respectively methyl group from V-AS as well as the excipients: microcrystalline cellulose, lactose monohydrate, croscarmellose, crospovidone, magnesium stearate;

– the increase (≈ 6% for P1), respectively the decrease (≈ 8% for P2) of the intensity for the band (≈ 1730 cm^{-1}) which represents the carbonyl vibration band from V-AS as well as the excipients: crospovidone, magnesium stearate;

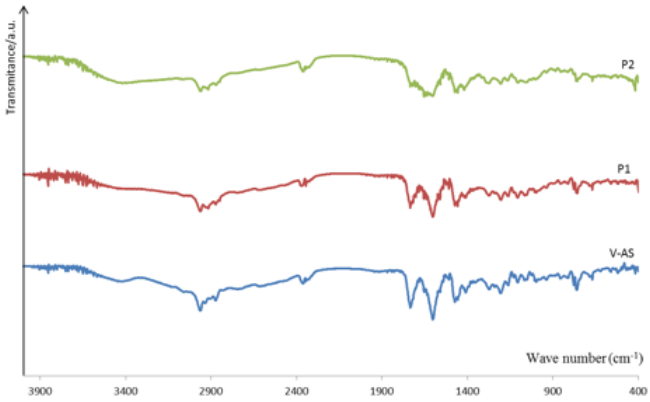

Fig. 5 FT-IR spectra

– the increase (≈ 4% for P1), respectively the decrease (≈ 10% for P2) for the most intense band (1603 cm^{-1}) which represents the vibration band of the groups C=N and C=C from V-AS as well as the excipients: crospovidone. For P2 the band appears with one shoulder at 1645 cm^{-1};

– the increase (≈ 13% for P1 and ≈ 9% for P2) of the intensity for the two bands from region 1470-1410 cm^{-1} that correspond to the COO (asymmetric, respectively symmetric) vibrations, respectively C-C ring stretching and N=N vibrations from V-AS as well as the excipients;

– the increase (≈ 12-16%) of the intensity for the three bands from the region 1280 -1160 cm^{-1} that correspond to the methyn, methylene, methyl and C-N vibrations from V-AS as well as the excipients;

– the significant increase (≈ 20%) of the intensity for the four bands from the region 1105 - 940 cm^{-1} that correspond to the C-O and C-C vibrations, respectively in p. and o.p. C-H band from V-AS as well as the excipients;

– the increasing (≈ 10%) of the intensity for the three bands from the region 853 -758 cm^{-1} that correspond to the vibrations of Si-O, o. p. C-H (ring) and o.p. C-H band from V-AS as well as the excipients;

– the increasing (≈ 15%) of the intensity of band from the region 669- 677 cm^{-1} that correspond to the vibrations of o. p. (ring) C-H band, o.p. N-H band and o.p. O-H band from V-AS as well as the excipients.

According to the differences that have been presented, the studied compounds may be considered to have a different composition.

X-ray analysis

In addition to the thermal method and FT-IR spectroscopy, X-ray powder diffraction was used in this study.

The emergence of new lines or the disappearance of diffractogram lines from the V-AS diffractogram,

Valsartan		P1		P2	
2teta	I%	2teta	I%	2teta	I%
		13.00	27.71		
		13.80	37.82	13.74	37.18
14.74	70.45	14.57	38.84	14.78	50.16
				16.85	45.37
17.45	67.61				
18.84	73.92				
				19.25	66.00
19.78	81.37	19.58	40.93	19.73	64.19
20.31	80.46	20.38	57.22	20.35	66.21
21.69	100	21.35	80.64		
		22.41	100	22.12	100
				23.41	59.34
		24.78	25.46		
26.58	43.12				

Table 2
X-RAY DIFFRACTIO DATA FOR V-AS, RESPECTIVELY P1 AND P2

respectively the change in intensity for certain lines, represent the differences between the studied compounds.

The X-ray diffraction data for the studied compounds are presented in table 2.

From the data presented in table 2, in case of pharmaceutical products can be observed that all the spectral lines have lower intensity, coupled with a small shift of all this lines at higher or lower diffraction angles. Simultaneously, it was observed the appearance of new lines, respectively the disappearance of some of the diffraction lines of higher and moderate intensities from V-AS.

These differences indicate a different composition between V-AS, respectively pharmaceuticals correspondent P1 and P2, as well as the possible interaction of V-AS with excipients at room temperature, which could increase with the increased temperature

Conclusions

The thermal stability of V-AS, respectively of the pharmaceutical products correspondents: P1 and P2, and indirectly the compatibility of V-AS with different excipients was studied by the thermal methods of analysis, the FT-IR spectroscopy and X-ray diffraction patterns.

The results confirmed that thermal analysis is an effective and reliable technique in the stability and compatibility studies of drug-excipient mixtures. Moreover, the DSC technique offers significant advantages, so that it is considered as a fast screening tool for drug-excipient interaction in preservation period.

The changes in the profile of thermoanalytical curves (TG/DTG and DSC) in the case of pharmaceutical compounds indicate the production of some interactions as a function of heating.

Because, the presence of solid-solid interaction does not necessary indicate pharmaceutical incompatibility, other analytical techniques were also used, such as FT-IR and XRPD, which can help in the interpretation of thermal results generally, respectively of DSC results particularly, in order to confirm the changes observed in drug-excipients curves.

References

1. COZLEA D.L., FARCAS D.M., VARI C., KERESZTESI A.A., ÞIFREA R., COZLEA L., DOGARU G., Farmacia, 61(4), 2013, p. 713
2. MITKOVA Z., VASILEVA M., SAVOVA A., MANOVA M., PETROVA G., Farmacia, 64(4), 2016, p. 633
3. AHJEL SW, LUPULEASA D, Farmacia, 57(3), 2009, p. 290
4. HANGAN A.C., TURZA A., STAN R.L., STEFAN R., OPREAN L.S., Russian Journal of Coordination Chemistry, 41(6), 2015, p. 365
5. OLARIU I., CONEAC G., VLAIA L., VLAIA V., ANGHEL D. F., ILIE C., POPOIU C., LUPULEASA D., Digest Journal of Nanomaterials and Biostructures, 9(1), 2014, p. 395
6. ***, Farmacopeea Romana, Ed. a X-a, Editura Medicala, Bucuresti, 2008
7. DRAGOMIROIU G.T.A.B., GINGHINA O., MIRON D.S., BARCA M., POPA D.E., HIRJAU M., LUPULEASA D., RADULESCU F.S., Farmacia, 63(2), 2015, p. 280
8. ***, European Pharmacopoeia, 9th Edition, Council of Europe, Strasbourg, 2017
9. HERMIDA R.C., CALVO C., AYALA D.E., MOJON A., RODRIGUEZ M., CHAYAN L., Chronobiol Int. 22, 2005, p. 755
10. SOOD J., SAPRA B., TIWARY A.K., AAPS PharmSciTech, 18(6), 2017, p. 1901
11. HANGAN A., BODOKI A., OPREAN L., CRISAN O., MIHALCA I., Farmacia, 60(6), 2012, p. 932
12. YASAM V.R., JAKKI S.L., NATARAJAN J., VENKATACHALAM S., KUPPUSAMY G., SOOD S., Drug Deliv., 23, 2016, p. 619
13. PARMAR B., MANDAL S., PETKAR K., PATEL L., SAWANT K., Int J Pharm Sci Nanotechnol., 4, 2011, p. 1483
14. YAN Y.D., SUNG J.H., KIM K.K., KIM D.W., KIM J.O., LEE B.J, Int J Pharm. 422(1), 2012, p. 202
15. NEKKANTI V., WANG Z., BETAGERI G.V., AAPS PharmSciTech, 17(4), 2016, DOI: 10.1208/s12249-015-0388-8
16. SALVIO N.H., BARROS P.A.F., DE SOUZA CARVALHO M.F., MATOS R.J., J Therm Anal Calorim. 102, 2010, p. 277
17. FELIX S.F., DA SILVA C.C.L., ANGNES L., MATOS R.J., J Therm Anal Calorim. 95, 2009, p. 877
18. MACEDO O.R., ARAGAO S.F.C., DO NASCIMENTO G.T., MACEDO C.M.A., J Therm Anal Calorim. 56, 1999, p. 1323
19. MACEDO O.R., DE SOUZA G.A., MACEDO C.M.A., J Therm Anal Calorim. 49, 1997, p. 937
20. NUNES S.R., SEMAAN S.F., RIGA T.A., CAVALHEIRO G.T.E., J Therm Anal Calorim. 97, 2009, p. 349
21. FREIRE D.F., ARAGAO S.F.C., DE LIMA A.F.T., RAFFIN N.F.M., J Therm Anal Calorim. 97, 2009, p. 355
22. MURA P., GRATTERI P., FAUCCI T.M., J Therm Anal Calorim. 68, 2002, p. 541
23. OLIVEIRA G.G.G., FERRAZ G.H., MATOS R.S.J., J Therm Anal Calorim. 79, 2005, p. 267
24. TITA, B., JURCA, T., RUSU, G., BANDUR, G., TITA, D., Rev Chim (Bucharest), **64**, no. 10, 2013, p. 1089
25. TITA, B., FULIAS, A., TITA, D., Rev Chim (Bucharest), **61**, no. 11, 2010, p. 1037
26. TITA ,B., MARIAN, E., FULIAS, A., JURCA ,T., TITA, D., J Therm Anal Calorim. **112**, 2013, p. 367
27. TITA, B., FULIAS, A., STEFANESCU, M., MARIAN, E., TITA, D., Rev Chim (Bucharest). **62**, no.2, 2011, p. 216
28. TITA, D., FULIAS, A, TITA, B., J Therm Anal Calorim. **111**, 2013, p. 1979
29. TITA, B., FULIAS, A., STEFANESCU, M., MARIAN, E. TITA, D., Rev Chim (Bucharest). **62,** no. 1, 2011, p. 31
30. TITA, B., JURCA, T., TITA, D., J Therm Anal Calorim. **113**, 2013, p. 291

Manuscript received: 12.10.2016